Supplement of Hydrol. Earth Syst. Sci., 28, 2123–2137, 2024
https://doi.org/10.5194/hess-28-2123-2024-supplement

Hydrology and Earth System Sciences
Open Access
EGU

Supplement of

Global total precipitable water variations and trends over the period 1958–2021

Nenghan Wan et al.

Correspondence to: Xiaomao Lin (xlin@ksu.edu)

Supplement Main text

S1.1 The relationship of T_s and T_{2m}

The comparison of long-term changes between T_s and T_{2m} in reanalyses over the ocean, land and globe as shown in Figure S4. T_s and T_{2m} show very similar interannual variations although some discrepancies exist in years, especially prior to the 1980s. The two are much closer thereafter when multiple satellite observations are assimilated in reanalyses, indicating the overall coupling between T_s and T_{2m}. In addition, the correlation of T_s and T_{2m} is strong (>0.9) and the trends aren't significantly different (student t-test) over ocean, land, and globe regions. For the variability over different latitude bins in Fig. S5 the discrepancy is the largest over polar area, with values around 0.4 K in JRA-55 and 0.2 K in ERA5. The difference between T_s and T_{2m} decrease after 1979 as more observations become available. Meanwhile, the trends of T_s and T_{2m} for the same latitude region aren't significantly different.

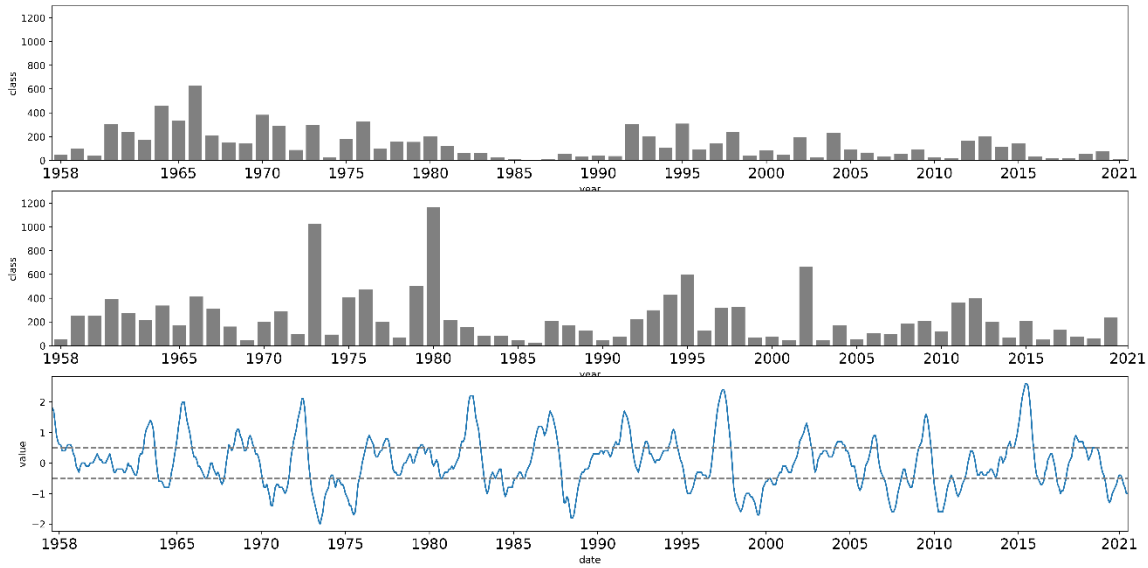

Figure S1. Detected change points for monthly temperature during 1958-2021 in (a) ERA5 and (b) JRA55. (c) The timeseries of Oceanic Niño Index (ONI) from 1958 to 2021. There is a total 21,307 of grids for PMF-test over the ocean.

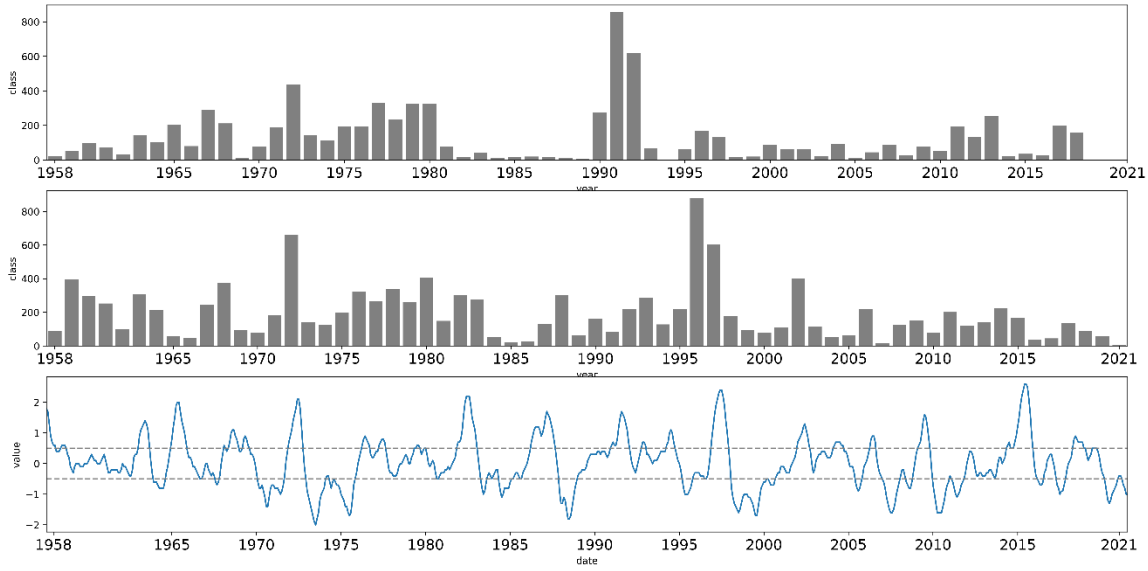

Figure S2. Histogram of years with detected change points for total precipitable water in ERA5 (a) and JRA-55 (b). (c) The timeseries of Oceanic Niño Index (ONI) from 1958 to 2021.

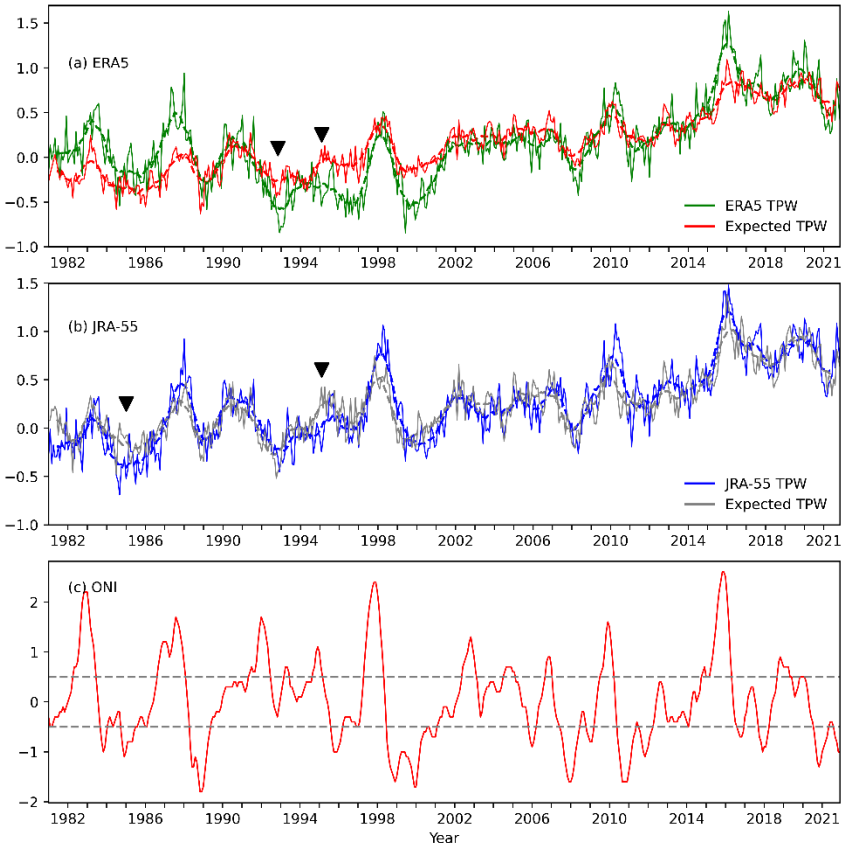

Figure S3. The variability of TPW and expected TPW calculated from regression with temperature for ERA5 (a) and JRA-55 (b). (c) The timeseries of Oceanic Niño Index (ONI) index from 1981 to 2021. Discrepancies are marked by triangles.

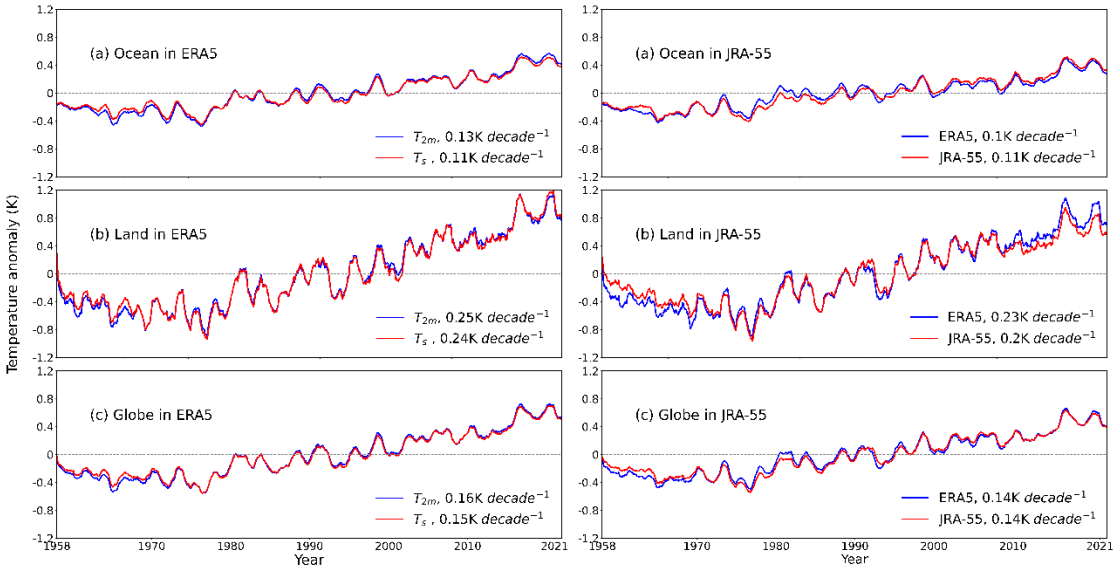

Figure S4. The relationship of monthly T_{2m} and T_s over land, ocean, and global for EAR5 (first column) and JRA-55 (second column).

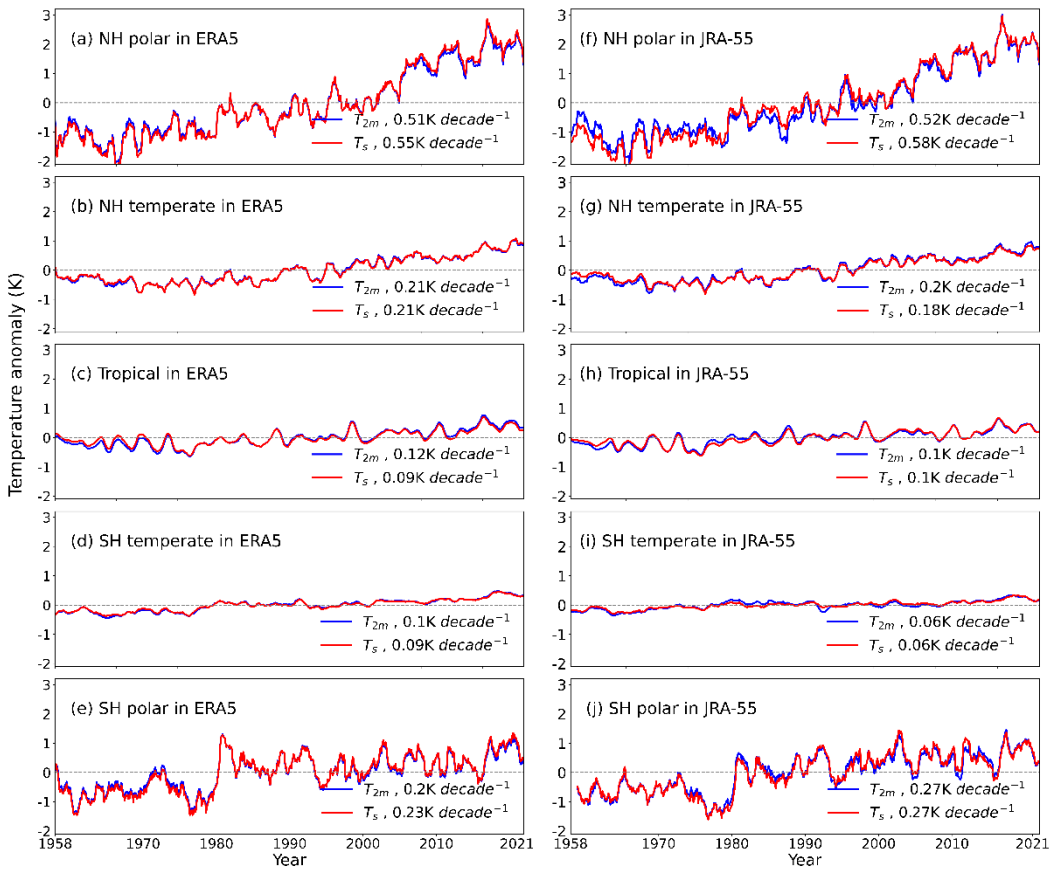

Figure S5. The same as Figure R4 but for (a) the Northern Hemisphere (NH) polar, (b) NH temperate, (c) Tropical, (d) Southern Hemisphere (SH) temperate, and (e) SH polar.

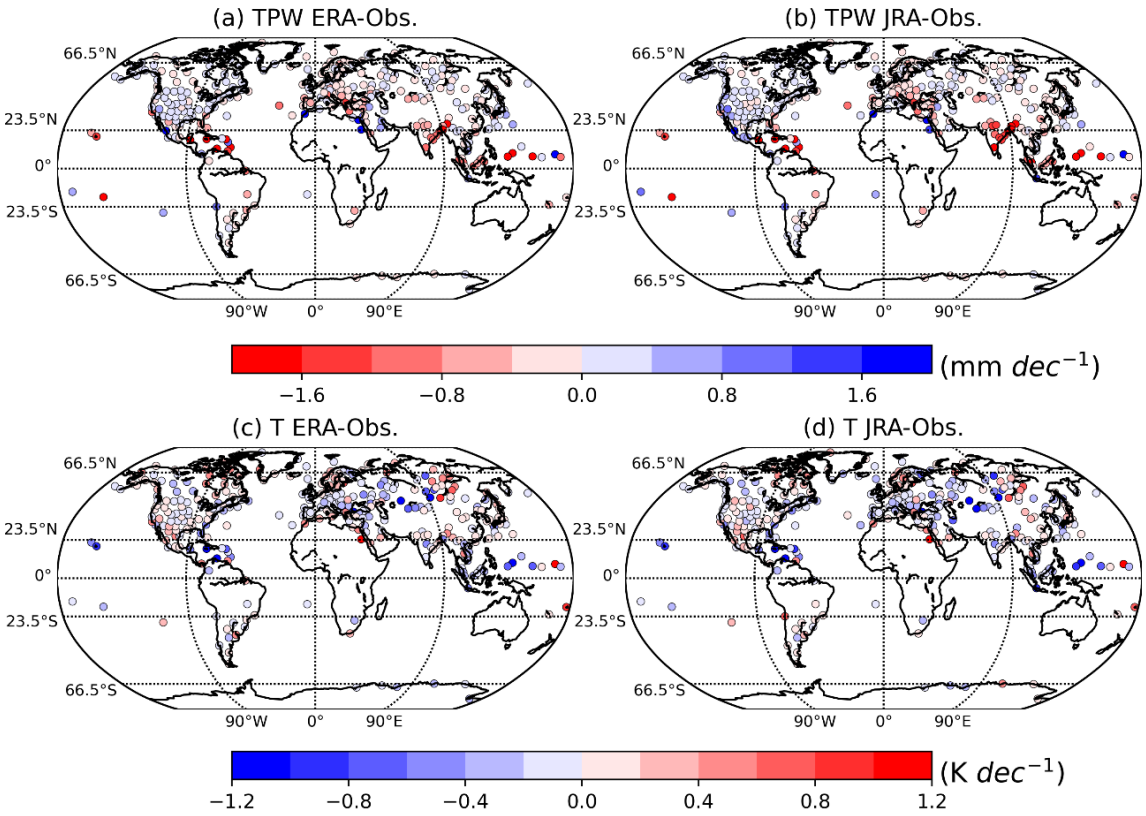

Figure S6. Trend comparisons with radiosondes: **(a-b)** TPW trends' difference (mm dec^{-1}) between radiosonde observations and ERA5 and JRA-55 from 1979-2019. **(c-d)** Same as **(a-b)** but for temperature trends' difference (K dec^{-1}). A total of 331 radiosonde observations were used in the analysis.

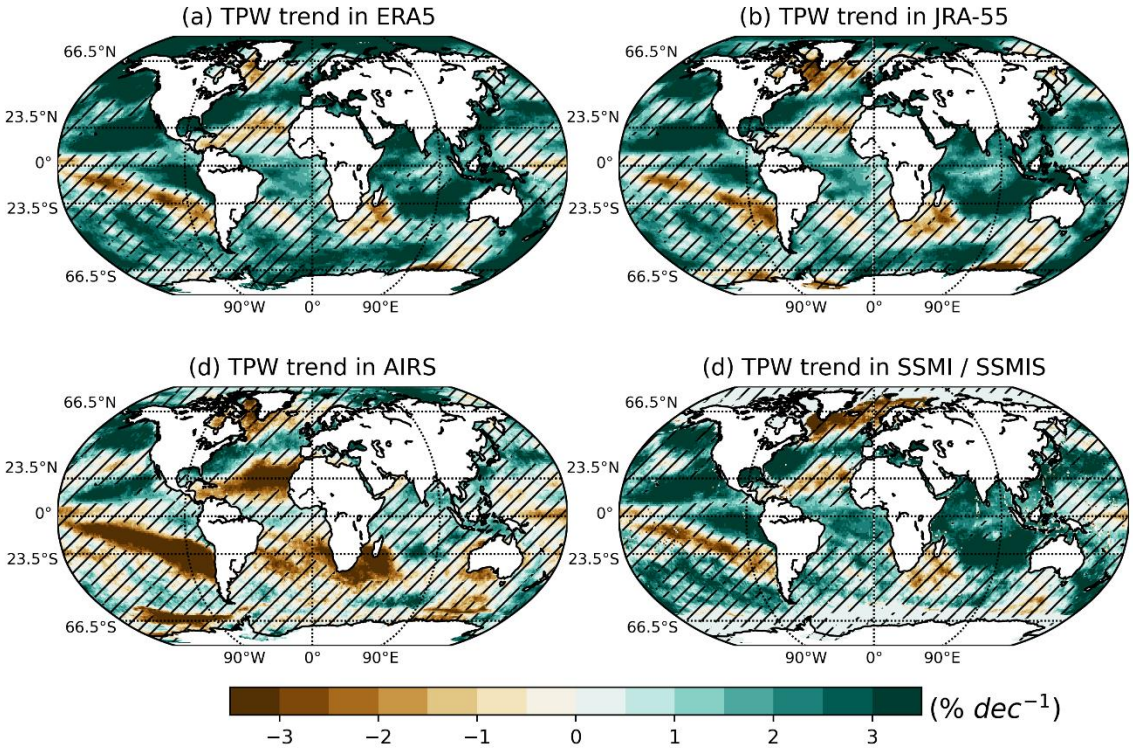

Figure S7. Trend comparisons with satellite observations from 2003-2021: Total precipitable water (TPW) trends over oceans for **(a)** ERA5, **(b)** JRA-55, **(c)** AIRS satellite, and **(d)** SSMI satellite. The hatch areas represent trends that are not significant at a 95% confidence level.